

Light nuclei photoproduction in relativistic heavy ion ultraperipheral collisions

Jin-Yu Hu,^{1,*} Shuo Lin,^{1,†} Shi Pu,^{1,2,‡} and Qun Wang^{1,3,§}

¹*Department of Modern Physics, University of Science and Technology of China, Anhui 230026, China*

²*Southern Center for Nuclear-Science Theory (SCNT), Institute of Modern Physics, Chinese Academy of Sciences, Huizhou 516000, Guangdong Province, China*

³*School of Mechanics and Physics, Anhui University of Science and Technology, Huainan, Anhui 232001, China*

We have investigated light nuclei pair photoproduction in relativistic heavy ion ultraperipheral collisions. As a first attempt, we employ our previously developed quantum electrodynamics model, which incorporates a wave-packet description of initial nuclei, to compute the cross section for proton-antiproton pair photoproduction. The effective vertex for the photon and proton interaction is chosen based on studies of two-photon exchange effects in hadron physics. We present the transverse momentum, invariant mass, and azimuthal angle distributions of proton-antiproton pairs at $\sqrt{s_{NN}} = 200$ GeV in Au+Au ultraperipheral collisions. We observe a $\cos(2\phi)$ modulation and an almost negligible $\cos(4\phi)$ modulation in the azimuthal angle distribution. Our studies helps us better understand the matter generated by light.

I. INTRODUCTION

In relativistic heavy ion collisions, two heavy nuclei are accelerated to near the speed of light, collide, and generate extremely strong electromagnetic fields on the order of $10^{17} - 10^{18}$ Gauss [1–3]. Although these fields decay rapidly in a vacuum, they can persist for a long time after interacting with the medium generated by the collisions [4–9]. Such strong fields provide a novel platform to study quantum transport phenomena (see Refs. [10–12] for recent reviews), the Schwinger mechanism [13–16], and photon-nuclear and photon-photon interactions. In the early 20th century, Fermi [17] first suggested, and Williams [18] and Weizsäcker [19] later improved, the idea that strong electromagnetic fields can be regarded as a flux of quasi-real photons. In relativistic heavy ion collisions, photon fluxes are significantly enhanced due to the large nuclear charge number. Additionally, the virtuality of photons is highly suppressed by the Lorentz factor, meaning the photons generated by the moving nuclei can be considered real. Therefore, relativistic heavy ion collisions offer a new opportunity to investigate photon-nuclear and photon-photon interactions.

Photon-nuclear interactions in high-energy scenarios, known as the photoproduction of vector mesons, have been recently measured in relativistic heavy ion ultraperipheral collisions (UPCs), e.g. see the measurements from RHIC-STAR [20–22] and LHC-ALICE experiments [23–25]. In the photoproduction of vector mesons, either nucleus can emit a photon while the other acts as a target, and vice versa. These two possibilities combine at the amplitude level and produce an interference effect, akin to a high-energy version of the double-slit interference phenomenon. This interference phenomenon was

recently observed in UPCs [22] as a significant breakthrough. Theoretical studies have discussed this phenomenon using the color glass condensate effective theory [26–28] and the vector meson dominance model [29]. This phenomenon has also been found to detect nuclear deformation effects in isobaric collisions [30, 31]. Another interesting photon-nuclear interaction is the photoproduction of di-jets, which has been measured at LHC-CMS [32] and discussed using Wigner distributions [33] or diffractive transverse momentum-dependent parton distribution functions of gluons [34].

The two key processes for photon-photon interactions in UPCs are light-by-light scattering, measured by LHC-ATLAS [35], and lepton pair photoproduction, measured by RHIC-STAR [20, 36], LHC-ATLAS [37] and LHC-ALICE experiments [38]. Since the photon generated by the moving nuclei is nearly real, as mentioned, lepton pair photoproduction in relativistic heavy ion collisions can also be considered as the Breit-Wheeler processes [39]. Although early pioneering works proposed the equivalent photon approximation [40–43], it has been found inadequate to accurately describe lepton pair photoproduction in UPCs due to its lack of dependence on impact parameters and the transverse momentum of the initial photons. Several theoretical methods have been developed to address photon-photon interactions in UPCs, including the generalized equivalent photon approximation and quantum electrodynamics (QED) in the background field approach [44–53], methods based on the factorization theorem [54–58], and QED models incorporating a wave-packet description of nuclei [59–61]. Higher-order effects, such as Coulomb corrections [55, 62–70] and Sudakov effects [52, 54–56, 71, 72], have also been considered. For further discussion, see the recent review [73] and references therein.

The successful discovery of the Breit-Wheeler process in UPCs naturally raises the question: could we observe the photoproduction of other particle-antiparticle pairs in UPCs? In this work, we study light nuclei pair photoproduction in UPCs using a QED model that incorporates a wave-packet description of nuclei [59–61]. As a

* jinyuhu2000@mail.ustc.edu.cn

† linshuo@mail.ustc.edu.cn

‡ shipu@ustc.edu.cn

§ qunwang@ustc.edu.cn

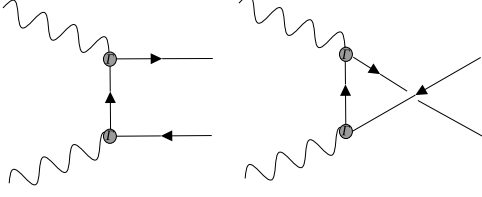


Figure 1. The Feynman diagram for the particle and anti-particle pairs in two photon fusion processes at Born level.

first attempt, we compute the cross section for proton-antiproton ($p\bar{p}$) pairs, the lightest nuclei, at the Born level. The effective photon-proton vertex is chosen following Refs. [74, 75]. We present results for the transverse momentum, invariant mass, and azimuthal angle distributions of $p\bar{p}$ pairs. Recently, we also notice the related work on $\gamma + \gamma \rightarrow p + \bar{p}$ through a different schemes [76] and $\gamma + \gamma \rightarrow \pi^+ + \pi^-$ in $e^+ + e^-$ collisions [77].

The paper is organized as follows. In Sec. II, we briefly review our theoretical formula for the differential cross section in UPCs. In Sec. III, we present the transverse momentum, invariant mass, and azimuthal angle distributions for $p\bar{p}$ pairs photoproduction at $\sqrt{s_{NN}} = 200$ GeV in UPCs. We summarize our work and discuss the results in Sec. IV.

II. THEORETICAL FRAMEWORK

We first review the theoretical framework for calculating the differential cross section of particle and antiparticle pair photoproduction. The framework follows Refs. [59, 60], in which some of us derived the differential cross section of lepton pair photoproduction using the classical field approximation with a wave packet description of nuclei. Consider two identical nuclei A_1 and A_2 move in $\pm z$ direction with the velocity $u_{1,2}^\mu = \gamma(1, 0, 0, \pm v)$, where $\gamma = 1/\sqrt{1-v^2}$ is the Lorentz factor. We can use a wave packet description for the initial nuclei. The sub-process involves two photons from the colliding nuclei producing a particle-antiparticle pair, described by

$$\gamma(p_1) + \gamma(p_2) \rightarrow H(k_1) + \bar{H}(k_2), \quad (1)$$

where p_1^μ and p_2^μ are four-momenta of photons, and $k_1^\mu = (E_{k_1}, \mathbf{k}_1)$ and $k_2^\mu = (E_{k_2}, \mathbf{k}_2)$ are on-shell four-momenta for particle H and anti-particle \bar{H} , respectively. The Born-level total cross section can be expressed in a compact form [59, 60],

$$\begin{aligned} \sigma &= \frac{Z^4 e^4}{2\gamma^4 v^3} \int d^2\mathbf{b}_T d^2\mathbf{b}_{1T} d^2\mathbf{b}_{2T} \delta^{(2)}(\mathbf{b}_T - \mathbf{b}_{1T} + \mathbf{b}_{2T}) \\ &\times \int \frac{d\omega_1 d^2\mathbf{p}_{1T}}{(2\pi)^3} \frac{d\omega_2 d^2\mathbf{p}_{2T}}{(2\pi)^3} \end{aligned}$$

$$\begin{aligned} &\times \int \frac{d^2\mathbf{p}'_{1T}}{(2\pi)^2} e^{-i\mathbf{b}_{1T} \cdot (\mathbf{p}'_{1T} - \mathbf{p}_{1T})} \frac{F^*(-\bar{p}'_1)}{-\bar{p}'_1} \frac{F(-\bar{p}_1)}{-\bar{p}_1} \\ &\times \int \frac{d^2\mathbf{p}'_{2T}}{(2\pi)^2} e^{-i\mathbf{b}_{2T} \cdot (\mathbf{p}'_{2T} - \mathbf{p}_{2T})} \frac{F^*(-\bar{p}'_2)}{-\bar{p}'_2} \frac{F(-\bar{p}_2)}{-\bar{p}_2} \\ &\times \int \frac{d^3k_1}{(2\pi)^3 2E_{k_1}} \frac{d^3k_2}{(2\pi)^3 2E_{k_2}} (2\pi)^4 \delta^{(4)}(\bar{p}_1 + \bar{p}_2 - k_1 - k_2) \\ &\times \sum_{\text{spin of } l, \bar{l}} [u_{1\mu} u_{2\nu} L^{\mu\nu}(\bar{p}_1, \bar{p}_2; k_1, k_2)] \\ &\times [u_{1\sigma} u_{2\rho} L^{\sigma\rho*}(\bar{p}'_1, \bar{p}'_2; k_1, k_2)], \quad (2) \end{aligned}$$

where Z is the proton number of the nuclei, \mathbf{b}_{iT} is the transverse position of the photon emission in nucleus A_i , \mathbf{b}_T is the impact parameter of colliding nuclei, \bar{p}_i and \bar{p}'_i are photon momenta in the classical field approximation and defined as ($i = 1, 2$ correspond to $+$ and $-$),

$$\bar{p}_i^\mu = \left(\omega_i, \mathbf{p}_{iT}, \pm \frac{\omega_i}{v} \right), \quad \bar{p}'_i^\mu = \left(\omega_i, \mathbf{p}'_{iT}, \pm \frac{\omega_i}{v} \right), \quad (3)$$

respectively. The form factor $F(-p^2)$ is the Fourier transform of the nuclear charge density distribution. In this work, we choose the form factor as in Ref. [40]

$$F(p) = \frac{4\pi\rho^0}{p^3} [\sin(pR_A) - pR_A \cos(pR_A)] \frac{1}{a^2 p^2 + 1}, \quad (4)$$

where $a = 0.7$ fm, $\rho^0 = 3A/(4\pi R_A^3)$ is the normalization factor, A is the number of nucleons in the nucleus, $R_A = 1.1A^{1/3}$ fm is the nucleus radius.

The tensor $L^{\mu\nu}$ in Eq. (2) depends on the final states generated through photoproduction. The typical Feynman diagrams for particle-antiparticle pairs in two-photon fusion processes at the Born level are presented in Fig. 1. If the particle H is a fermion, then the effective $L^{\mu\nu}$ can be written in a compact form,

$$\begin{aligned} &L^{\mu\nu}(p_1, p_2; k_1, k_2) \\ &= -\bar{u}(k_1) [\Gamma^\mu S_F(k_1, p_1) \Gamma^\nu + \Gamma^\nu S_F(p_1, k_2) \Gamma^\mu] v(k_2), \quad (5) \end{aligned}$$

where S_F is the effective propagator and Γ^μ is the effective vertex, which will reduce to γ^μ in lepton pair photoproduction [59, 60].

Now, let us consider light nuclei photoproduction. As a first attempt, we consider the photoproduction of the lightest nuclei and anti-nuclei pair, i.e., $p\bar{p}$ pairs. Since light nuclei are not elementary particles, the effective vertex Γ^μ and the effective propagator S_F must be chosen based on phenomenological models. The photon-proton interactions are widely discussed in the context of two-photon exchange effects in $e^- + p \rightarrow e^- + p$ and $e^+ + e^- \rightarrow p + \bar{p}$ [74, 75, 78, 79], also see recent review [80, 81] and references therein. Several methods are also proposed to detect the two two-photon exchange effects in experiments [82–84].

Therefore, here, we adopt the fermionic propagator $S_F(k, p)$ in the lowest order of perturbative theory,

$$-iS_F(k, p) = \frac{\gamma \cdot (k - p) + m_p}{(k - p)^2 - m_p^2 + i\epsilon}, \quad (6)$$

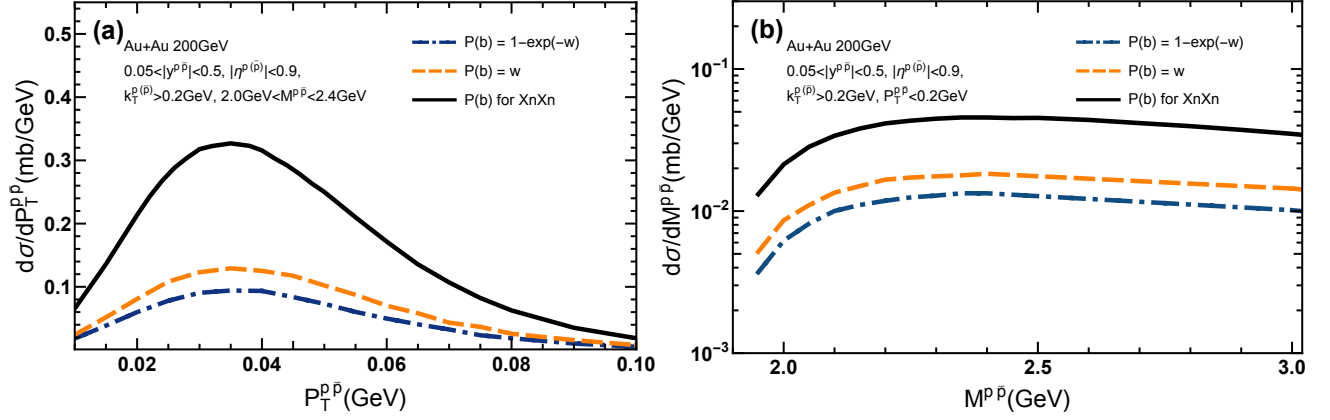


Figure 2. Differential cross sections as functions of (a) transverse momentum $P_T^{p\bar{p}}$, (b) invariant mass $M^{p\bar{p}}$ for $p\bar{p}$ pairs. Different lines represent results computed with different $\mathcal{P}(b_T)$. The black solid lines use $\mathcal{P}(b_T)$ from Eq. (10) with w from Eq. (12). The orange dashed lines use $\mathcal{P}(b_T)$ from Eq. (11) with w from Eq. (12). The blue dotted lines use $\mathcal{P}(b_T)$ from Eq. (11) with w from Eq. (12).

with m_p being the mass of proton and we follow Ref.[78] to adopt,

$$\Gamma^\mu(q) = F_1(q^2)\gamma^\mu + i\frac{F_2(q^2)}{2m_p}\sigma^{\mu\nu}q_\nu, \quad (7)$$

where $\sigma^{\mu\nu} = i[\gamma^\mu, \gamma^\nu]/2$ and F_1 and F_2 are related to the Sachs form factors G_E and G_M ,

$$\begin{aligned} F_1(q^2) &= \frac{G_E(q^2) + \tau G_M(q^2)}{1 + \tau}, \\ F_2(q^2) &= \frac{G_M(q^2) - G_E(q^2)}{1 + \tau}, \end{aligned} \quad (8)$$

with $\tau = -q^2/4m_p^2$. The form factors G_E and G_M are commonly parameterized as,

$$G_E(q^2) = \frac{G_M(q^2)}{\mu_p} = -\frac{\Lambda^2}{q^2 - \Lambda^2}, \quad (9)$$

with μ_p being the magnetic moment of proton and $\Lambda = 0.84$ GeV [78]. In general, particle-antiparticle pairs can also be generated through the s -channel. However, this contribution may strongly depend on the effective coupling constant and is usually found to be smaller than that of the current scheme (also see Ref. [76] for related discussions).

In RHIC-STAR experiments, the UPC events are triggered by detecting the neutrons emitted from nuclei-photon interactions. To compare with experimental data, we further need to add an extra factor $\mathcal{P}^2(b_\perp)$ in the cross sections. The $\mathcal{P}(b_\perp)$ is the probability of emitting neutrons from the excited nucleus and can usually be parameterized as [41],

$$\mathcal{P}(b_T) = 1 - \exp(-w), \quad (10)$$

where w is a function of b_T . When w is small, $\mathcal{P}(b_T)$ in Eq. (10) is also approximately given by [47],

$$\mathcal{P}(b_\perp) \simeq w. \quad (11)$$

Table I. The total cross section for $p\bar{p}$ pair photoproduction with different choices of $\mathcal{P}(b_T)$ at $\sqrt{s_{NN}} = 200$ GeV and 54 GeV in Au+Au UPCs. We have chosen $k_{1T}, k_{2T} \geq 200$ MeV, $|y^{p\bar{p}}| \in [0.05, 0.5]$ and $\eta^{p\bar{p}} \in [-0.9, -0.9]$. The errors from the numerical integration are estimated by ZMCintegral package.

$\sqrt{s_{NN}}$	$\mathcal{P}(b_T) = 1 - e^{-w}$	$\mathcal{P}(b_T) = w$	$\mathcal{P}(b_T)$ for XnXn
200 GeV	$4.5 \pm 0.1 \mu\text{b}$	$6.3 \pm 0.1 \mu\text{b}$	$15.7 \pm 0.3 \mu\text{b}$
54 GeV	$51 \pm 3 \text{nb}$	$78 \pm 4 \text{nb}$	$170 \pm 1 \text{nb}$

One popular way to estimate w is to use the Giant Dipole Resonance model [41, 47, 68, 85],

$$w = 5.45 \times 10^{-5} Z^3 (A - Z) / (A^{2/3} b_T^2). \quad (12)$$

Since w in Eq. (12) only depends on A, Z and b_T , the details of the nuclear mass distribution or deformation effects are missing in this model. Another way to derive w is to use the equivalent photon approximation [50, 68, 86–89],

$$w_{Xn}(b_T) = \int d\omega n(\omega, b_T) \sigma_{\gamma+A \rightarrow A'+Xn}(\omega), \quad (13)$$

where the $X \geq 1$ stands for the number of neutrons emitted by a nucleus and $n(\omega, b_T)$ is the photon flux [45, 59, 90], and the photon-nucleus cross section $\sigma_{\gamma+A \rightarrow A'+Xn}$ is given by fixed-target experiments [86, 91, 92]. In this work, we consider three kinds of $\mathcal{P}(b_T)$, (i) $\mathcal{P}(b_T)$ from Eq. (10) with w from Eq. (12), labeled as “ $\mathcal{P}(b_T) = 1 - \exp(-w)$ ”, (ii) $\mathcal{P}(b_T)$ from Eq. (11) with w from Eq. (12), labeled as “ $\mathcal{P}(b_T) = w$ ”, (iii) $\mathcal{P}(b_T)$ from Eq. (10) with w from Eq. (13), labeled as “XnXn”. These labels are used in the following figures.

III. TRANSVERSE MOMENTUM, INVARIANT MASS SPECTRUM AND AZIMUTHAL ANGLE DISTRIBUTIONS

In this section, we present numerical results for the transverse momentum, invariant mass, and azimuthal angle distributions of $p\bar{p}$ pair photoproduction in Au+Au UPCs. We define $\mathbf{P}_T^{p\bar{p}} = \mathbf{k}_{1T} + \mathbf{k}_{2T}$ as the transverse momentum of the $p\bar{p}$ pair, where \mathbf{k}_{1T} and \mathbf{k}_{2T} are the transverse momentum of p and \bar{p} , respectively, as introduced in Eq. (2). Additionally, we also define $M^{p\bar{p}}$, ϕ , and $y^{p\bar{p}}$ as the invariant mass of the $p\bar{p}$ pair, the angle between $\mathbf{P}_T^{p\bar{p}}$ and $\frac{1}{2}(\mathbf{k}_{2T} - \mathbf{k}_{1T})$, the rapidity of $p\bar{p}$ pair. We use $\eta^{p(\bar{p})}$ for pseudo-rapidity of single p or \bar{p} . We set $\mathbf{k}_{1T}, \mathbf{k}_{2T} \geq 200$ MeV, $|y^{p\bar{p}}| \in [0.05, 0.5]$ and $\eta^{p(\bar{p})} \in [-0.9, 0.9]$. The high dimensional integration in Eq. (2) is computed by ZMCintegral package [93, 94].

We first present the total cross section for $p\bar{p}$ pairs photoproduction at the $\sqrt{s_{NN}} = 200$ GeV and 54 GeV in Au+Au UPCs with the different choice of $\mathcal{P}(b_T)$ in Table I. We observe that the total cross section are consistently in the range of $\sim 4 - 10\mu\text{b}$ at $\sqrt{s_{NN}} = 200$ GeV and $\sim 50 - 170$ nb at $\sqrt{s_{NN}} = 54$ GeV, respectively.

The differential cross section as a function of transverse momentum $\mathbf{P}_T^{p\bar{p}}$ for $p\bar{p}$ pairs is shown in Fig. 2(a). We observe that the $d\sigma/d\mathbf{P}_T^{p\bar{p}}$ ranges from 0.1 to 0.3 mb/GeV, with peaks around 0.035 – 0.040 GeV. The differential cross section with $\mathcal{P}(b_T)$ from XnXn is slightly higher than those from the other two forms of $\mathcal{P}(b_T)$.

We also plot the invariant mass $M^{p\bar{p}}$ distribution of $p\bar{p}$ pairs in Fig. 2(b). Interestingly, the differential cross section grows smoothly when $M^{p\bar{p}} < 2.4$ GeV, which contrasts with the rapid rise near the threshold seen in lepton pair photoproduction. This difference arises from the non-trivial effective electromagnetic form factors for protons in Eq. (7). For $M^{p\bar{p}} > 2.4$ GeV, the differential cross section decreases slowly. Therefore, further experimental measurements of $p\bar{p}$ pairs photoproduction can provide additional constraints on the effective vertex Γ^μ .

Finally, we plot the azimuthal angle distribution for $p\bar{p}$ pairs in Fig. 3. The azimuthal angle distribution for lepton pair production exhibits $\cos(4\phi)$ and $\cos(2\phi)$ modulation due to the linear polarization of initial photons [52, 56]. We fit the differential cross section $d\sigma/d\phi$ using the function $\mathcal{A}_0 + \mathcal{A}_2 \cos(2\phi) + \mathcal{A}_4 \cos(4\phi)$. The coefficients $\mathcal{A}_0, \mathcal{A}_2$ and \mathcal{A}_4 are shown in Table II. In previous studies of lepton pair photoproduction [52, 56, 60], it was found that the $\cos(2\phi)$ modulation is proportional to the mass squared of leptons. It was observed that dimuon pair photoproduction has a much larger $\cos(2\phi)$ modulation than dielectron production. Therefore, it is not surprising to observe $\cos(2\phi)$ modulation for $p\bar{p}$ pairs photoproduction, despite the significant differences in the vertex Γ^μ for protons in Eq. (7) compared to leptons. Interestingly, we do not observe significant $\cos(4\phi)$ modulation in Fig. 3, and \mathcal{A}_4 is always an order of magnitude smaller than \mathcal{A}_2 in Table II. Therefore, measurements of

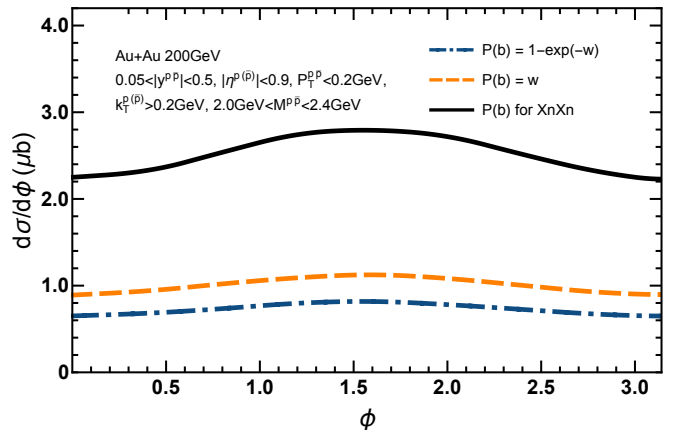


Figure 3. Differential cross sections as a function of azimuthal angle ϕ . The different lines have the same meanings as in Fig. 2.

Table II. We fit the $d\sigma/d\phi$ using the function $\mathcal{A}_0 + \mathcal{A}_2 \cos(2\phi) + \mathcal{A}_4 \cos(4\phi)$. The coefficients $\mathcal{A}_0, \mathcal{A}_2$ and \mathcal{A}_4 for different $\mathcal{P}(b_T)$.

	$\mathcal{A}_0(\mu\text{b})$	$\mathcal{A}_2(\mu\text{b})$	$\mathcal{A}_4(\mu\text{b})$
$\mathcal{P}(b_T) = 1 - e^{-w}$	0.73	-0.08	$\sim 10^{-3}$
$\mathcal{P}(b_T) = w$	1.01	-0.11	$\sim 10^{-3}$
$\mathcal{P}(b_T)$ for XnXn	2.52	-0.28	0.01

the azimuthal angle can also impose constraints on the vertex Γ^μ .

IV. CONCLUSION AND DISCUSSION

In this work, we studied light nuclei photoproduction in UPCs using our QED model that incorporates a wave-packet description of nuclei. As a first attempt, we considered the photoproduction of the lightest nuclei pairs, $p\bar{p}$ pairs, at the Born level in UPCs. The effective vertex between photons and protons, Γ^μ , was chosen based on studies of two-photon exchange effects, including information on the electromagnetic form factors of the proton. We then present the transverse momentum and invariant mass distributions of $p\bar{p}$ pairs at $\sqrt{s_{NN}} = 200$ GeV in UPCs in 2(a) and (b), respectively. Interestingly, we observe a significant $\cos(2\phi)$ modulation and an almost vanishing $\cos(4\phi)$ modulation in the azimuthal angle distribution of $p\bar{p}$ pairs in Fig. 3. Our study is closely linked to two-photon exchange effects in hadron physics. Therefore, further measurements in UPCs can also provide constraints on these effects.

Light nuclei photoproduction opens a new window to generate light nuclei and helps us better understand the matter generated by light. Following the similar strategy, one can also consider deuterium or helium nuclei photoproduction within our theoretical framework. For

deuterium nuclei, which are spin-1, the propagator in tensor $L^{\mu\nu}$ needs to be replaced accordingly, and the effective vertex may include contributions from the electric quadrupole moment. For helium nuclei, more complex nuclear information may be involved. Further discussions along this line will be presented elsewhere.

ACKNOWLEDGMENTS

We would like to thank Wang-Mei Zha, Xin Wu and Cheng Zhang for helpful discussion. This work is

supported in part by the National Key Research and Development Program of China under Contract No. 2022YFA1605500, by the Chinese Academy of Sciences (CAS) under Grants No. YSBR-088 and by National Nature Science Foundation of China (NSFC) under Grants No. 12075235, No. 12135011, No. 12275082, No. 12035006, and No. 12075085.

-
- [1] A. Bzdak and V. Skokov, *Phys. Lett.* **B710**, 171 (2012), 1111.1949.
- [2] W.-T. Deng and X.-G. Huang, *Phys. Rev.* **C85**, 044907 (2012), 1201.5108.
- [3] V. Roy and S. Pu, *Phys. Rev.* **C92**, 064902 (2015), 1508.03761.
- [4] V. Roy, S. Pu, L. Rezzolla, and D. Rischke, *Phys. Lett.* **B750**, 45 (2015), 1506.06620.
- [5] S. Pu, V. Roy, L. Rezzolla, and D. H. Rischke, *Phys. Rev.* **D93**, 074022 (2016), 1602.04953.
- [6] S. Pu and D.-L. Yang, *Phys. Rev.* **D93**, 054042 (2016), 1602.04954.
- [7] I. Siddique, R.-j. Wang, S. Pu, and Q. Wang, *Phys. Rev.* **D99**, 114029 (2019), 1904.01807.
- [8] G. Inghirami *et al.*, *Eur. Phys. J.* **C76**, 659 (2016), 1609.03042.
- [9] J.-J. Zhang *et al.*, *Phys. Rev. Res.* **4**, 033138 (2022), 2201.06171.
- [10] D. E. Kharzeev and J. Liao, *Nature Rev. Phys.* **3**, 55 (2021), 2102.06623.
- [11] J.-H. Gao, G.-L. Ma, S. Pu, and Q. Wang, *Nucl. Sci. Tech.* **31**, 90 (2020), 2005.10432.
- [12] Y. Hidaka, S. Pu, Q. Wang, and D.-L. Yang, *Prog. Part. Nucl. Phys.* **127**, 103989 (2022), 2201.07644.
- [13] J. S. Schwinger, *Phys. Rev.* **82**, 664 (1951), [116(1951)].
- [14] P. Copinger, K. Fukushima, and S. Pu, *Phys. Rev. Lett.* **121**, 261602 (2018), 1807.04416.
- [15] P. Copinger and S. Pu, *Int. J. Mod. Phys. A* **35**, 2030015 (2020), 2008.03635.
- [16] P. Copinger and S. Pu, (2022), 2203.00847.
- [17] E. Fermi, *Z. Phys.* **29**, 315 (1924).
- [18] E. J. Williams, *Phys. Rev.* **45**, 729 (1934).
- [19] C. F. von Weizsacker, *Z. Phys.* **88**, 612 (1934).
- [20] STAR, J. Adam *et al.*, *Phys. Rev. Lett.* **127**, 052302 (2021), 1910.12400.
- [21] STAR, M. Abdallah *et al.*, *Phys. Rev. Lett.* **128**, 122303 (2022), 2109.07625.
- [22] STAR, M. Abdallah *et al.*, *Sci. Adv.* **9**, eabq3903 (2023), 2204.01625.
- [23] ALICE, S. Acharya *et al.*, *Phys. Lett. B* **798**, 134926 (2019), 1904.06272.
- [24] ALICE, S. Acharya *et al.*, *JHEP* **06**, 035 (2020), 2002.10897.
- [25] ALICE, S. Acharya *et al.*, *Eur. Phys. J. C* **81**, 712 (2021), 2101.04577.
- [26] H. Xing, C. Zhang, J. Zhou, and Y.-J. Zhou, *JHEP* **10**, 064 (2020), 2006.06206.
- [27] Y. Hagiwara, C. Zhang, J. Zhou, and Y.-J. Zhou, *Phys. Rev. D* **103**, 074013 (2021), 2011.13151.
- [28] Y. Hagiwara, C. Zhang, J. Zhou, and Y.-j. Zhou, *Phys. Rev. D* **104**, 094021 (2021), 2106.13466.
- [29] W. Zha, J. D. Brandenburg, L. Ruan, Z. Tang, and Z. Xu, *Phys. Rev. D* **103**, 033007 (2021), 2006.12099.
- [30] H. Mäntysaari, F. Salazar, B. Schenke, C. Shen, and W. Zhao, *Phys. Rev. C* **109**, 024908 (2024), 2310.15300.
- [31] S. Lin, J.-Y. Hu, H.-J. Xu, S. Pu, and Q. Wang, (2024), 2405.16491.
- [32] CMS, A. Tumasyan *et al.*, *Phys. Rev. Lett.* **131**, 051901 (2023), 2205.00045.
- [33] Y. Hagiwara, Y. Hatta, R. Pasechnik, M. Tasevsky, and O. Teryaev, *Phys. Rev. D* **96**, 034009 (2017), 1706.01765.
- [34] E. Iancu, A. H. Mueller, D. N. Triantafyllopoulos, and S. Y. Wei, *Eur. Phys. J. C* **83**, 1078 (2023), 2304.12401.
- [35] ATLAS, M. Aaboud *et al.*, *Nature Phys.* **13**, 852 (2017), 1702.01625.
- [36] STAR, J. Adam *et al.*, *Phys. Rev. Lett.* **121**, 132301 (2018), 1806.02295.
- [37] ATLAS, M. Aaboud *et al.*, *Phys. Rev. Lett.* **121**, 212301 (2018), 1806.08708.
- [38] ALICE, S. Acharya *et al.*, **06**, 024 (2023), 2204.11732.
- [39] G. Breit and J. A. Wheeler, *Phys. Rev.* **46**, 1087 (1934).
- [40] S. R. Klein, J. Nystrand, J. Seger, Y. Gorbunov, and J. Butterworth, *Comput. Phys. Commun.* **212**, 258 (2017), 1607.03838.
- [41] C. A. Bertulani and G. Baur, *Phys. Rept.* **163**, 299 (1988).
- [42] C. A. Bertulani, S. R. Klein, and J. Nystrand, *Ann. Rev. Nucl. Part. Sci.* **55**, 271 (2005), nucl-ex/0502005.
- [43] A. J. Baltz, *Phys. Rept.* **458**, 1 (2008), 0706.3356.
- [44] X. Wang *et al.*, *Phys. Rev. C* **107**, 044906 (2023), 2207.05595.
- [45] M. Vidovic, M. Greiner, C. Best, and G. Soff, *Phys. Rev. C* **47**, 2308 (1993).
- [46] K. Hencken, D. Trautmann, and G. Baur, *Phys. Rev. A* **51**, 1874 (1995), nucl-th/9410014.
- [47] K. Hencken, G. Baur, and D. Trautmann, *Phys. Rev. C* **69**, 054902 (2004), nucl-th/0402061.
- [48] W. Zha, J. D. Brandenburg, Z. Tang, and Z. Xu, *Phys. Lett. B* **800**, 135089 (2020), 1812.02820.
- [49] W. Zha, L. Ruan, Z. Tang, Z. Xu, and S. Yang, *Phys. Lett. B* **781**, 182 (2018), 1804.01813.
- [50] J. D. Brandenburg *et al.*, (2020), 2006.07365.

- [51] J. D. Brandenburg, W. Zha, and Z. Xu, *Eur. Phys. J. A* **57**, 299 (2021), 2103.16623.
- [52] C. Li, J. Zhou, and Y.-J. Zhou, *Phys. Rev. D* **101**, 034015 (2020), 1911.00237.
- [53] J. Luo, X. Li, Z. Tang, X. Wu, and W. Zha, (2023), 2308.03070.
- [54] S. Klein, A. H. Mueller, B.-W. Xiao, and F. Yuan, *Phys. Rev. Lett.* **122**, 132301 (2019), 1811.05519.
- [55] S. Klein, A. H. Mueller, B.-W. Xiao, and F. Yuan, *Phys. Rev. D* **102**, 094013 (2020), 2003.02947.
- [56] C. Li, J. Zhou, and Y.-J. Zhou, *Phys. Lett. B* **795**, 576 (2019), 1903.10084.
- [57] B.-W. Xiao, F. Yuan, and J. Zhou, *Phys. Rev. Lett.* **125**, 232301 (2020), 2003.06352.
- [58] Y. Shi, L. Chen, S.-Y. Wei, and B.-W. Xiao, (2024), 2406.07634.
- [59] R.-j. Wang, S. Pu, and Q. Wang, *Phys. Rev. D* **104**, 056011 (2021), 2106.05462.
- [60] R.-j. Wang, S. Lin, S. Pu, Y.-f. Zhang, and Q. Wang, *Phys. Rev. D* **106**, 034025 (2022), 2204.02761.
- [61] S. Lin *et al.*, *Phys. Rev. D* **107**, 054004 (2023), 2210.05106.
- [62] D. Ivanov and K. Melnikov, *Phys. Rev. D* **57**, 4025 (1998), hep-ph/9709352.
- [63] U. Eichmann, J. Reinhardt, and W. Greiner, *Phys. Rev. A* **59**, 1223 (1999), nucl-th/9806031.
- [64] B. Segev and J. C. Wells, *Phys. Rev. A* **57**, 1849 (1998), physics/9710008.
- [65] A. J. Baltz and L. D. McLerran, *Phys. Rev. C* **58**, 1679 (1998), nucl-th/9804042.
- [66] A. J. Baltz, F. Gelis, L. D. McLerran, and A. Peshier, *Nucl. Phys. A* **695**, 395 (2001), nucl-th/0101024.
- [67] A. J. Baltz, *Phys. Rev. C* **68**, 034906 (2003), nucl-th/0305083.
- [68] A. J. Baltz, Y. Gorbunov, S. R. Klein, and J. Nystrand, *Phys. Rev. C* **80**, 044902 (2009), 0907.1214.
- [69] W. Zha and Z. Tang, (2021), 2103.04605.
- [70] Z.-h. Sun, D.-x. Zheng, J. Zhou, and Y.-j. Zhou, *Phys. Lett. B* **808**, 135679 (2020), 2002.07373.
- [71] D. Y. Shao, C. Zhang, J. Zhou, and Y.-j. Zhou, (2023), 2306.02337.
- [72] D. Y. Shao, C. Zhang, J. Zhou, and Y.-J. Zhou, *Phys. Rev. D* **107**, 036020 (2023), 2212.05775.
- [73] P. Shi, X. Bo-Wen, Z. Jian, and Z. Ya-Jin, *Acta Phys. Sin.* **72**, 072503 (2023).
- [74] J. Guttmann, N. Kivel, and M. Vanderhaeghen, *Phys. Rev. D* **83**, 094021 (2011), 1101.5967.
- [75] H. Q. Zhou, D. Y. Chen, and Y. B. Dong, *Phys. Lett. B* **675**, 305 (2009), 0903.0301.
- [76] C. Zhang, L.-M. Zhang, and D. Y. Shao, (2024), 2406.05618.
- [77] Y. Jia, J. Zhou, and Y.-j. Zhou, (2024), 2406.09381.
- [78] P. G. Blunden, W. Melnitchouk, and J. A. Tjon, *Phys. Rev. Lett.* **91**, 142304 (2003), nucl-th/0306076.
- [79] P. A. M. Guichon and M. Vanderhaeghen, *Phys. Rev. Lett.* **91**, 142303 (2003), hep-ph/0306007.
- [80] C. E. Carlson and M. Vanderhaeghen, *Ann. Rev. Nucl. Part. Sci.* **57**, 171 (2007), hep-ph/0701272.
- [81] J. Arrington, P. G. Blunden, and W. Melnitchouk, *Prog. Part. Nucl. Phys.* **66**, 782 (2011), 1105.0951.
- [82] PANDA, M. F. M. Lutz *et al.*, (2009), 0903.3905.
- [83] D. M. Nikolenko *et al.*, *Phys. Atom. Nucl.* **73**, 1322 (2010).
- [84] OLYMPUS, M. Kohl, *AIP Conf. Proc.* **1374**, 527 (2011).
- [85] G. Baur, K. Hencken, and D. Trautmann, *J. Phys. G* **24**, 1657 (1998), hep-ph/9804348.
- [86] A. J. Baltz, C. Chasman, and S. N. White, *Nucl. Instrum. Meth. A* **417**, 1 (1998), nucl-ex/9801002.
- [87] A. J. Baltz, S. R. Klein, and J. Nystrand, *Phys. Rev. Lett.* **89**, 012301 (2002), nucl-th/0205031.
- [88] M. Broz, J. G. Contreras, and J. D. Tapia Takaki, *Comput. Phys. Commun.* **253**, 107181 (2020), 1908.08263.
- [89] I. A. Pshenichnov, J. P. Bondorf, I. N. Mishustin, A. Ventura, and S. Masetti, *Phys. Rev. C* **64**, 024903 (2001), nucl-th/0101035.
- [90] J. D. Jackson, *Classical Electrodynamics* (Wiley, 1998).
- [91] A. Veyssiere, H. Beil, R. Bergere, P. Carlos, and A. Lepretre, *Nucl. Phys. A* **159**, 561 (1970).
- [92] B. L. Berman *et al.*, *Phys. Rev. C* **36**, 1286 (1987).
- [93] H.-Z. Wu, J.-J. Zhang, L.-G. Pang, and Q. Wang, *Comput. Phys. Commun.* **248**, 106962 (2020), 1902.07916.
- [94] J.-J. Zhang and H.-Z. Wu, *Comput. Phys. Commun.* **251**, 107240 (2020), 1910.01965.